GLOBAL MOON COVERAGE VIA HYPERBOLIC FLYBYS

Brent Buffington(1), **Nathan Strange**(2), **and Stefano Campagnola**(3)
(1) *Jet Propulsion Laboratory / California Institute of Technology, 4800 Oak Grove Drive, Pasadena, CA, 91109-8099, 818.393.7964, Brent.Buffington@jpl.nasa.gov*
(2) *Jet Propulsion Laboratory / California Institute of Technology, 4800 Oak Grove Drive, Pasadena, CA, 91109-8099, 818.393.1165, Nathan.Strange@jpl.nasa.gov*
(3) *JAXA/ISAS, Yoshinodai 3-1-1, chuo-ku, Sagamihara, Kanagawa, 252-5210, Japan*

Abstract: *The scientific desire for global coverage of moons such as Jupiter's Galilean moons or Saturn's Titan has invariably led to the design of orbiter missions. These orbiter missions require a large amount of propellant needed to insert into orbit around such small bodies, and for a given launch vehicle, the additional propellant mass takes away from mass that could otherwise be used for scientific instrumentation on a multiple flyby-only mission. This paper will present methods—expanding upon techniques developed for the design of the Cassini prime and extended missions—to obtain near global moon coverage through multiple flybys. Furthermore we will show with proper instrument suite selection, a flyby-only mission can provide science return similar (and in some cases greater) to that of an orbiter mission.*

Keywords: *gravity assist, trajectory design, mission design, and orbital mechanics.*

1. Introduction

Traditionally, the challenge of global coverage of moons such as Jupiter's Galilean moons or Saturn's Titan has led to the design of orbiter missions. Such orbiter missions are very expensive in propellant as a result of the large maneuver required insert into orbit around such small bodies, and can be plagued by orbit stability complexities. Furthermore, for a given launch vehicle, the large amount of propellant associated with orbit insertion takes away from mass that could otherwise be used for scientific instrumentation, and in the case of a Europa mission, shielding–in the form of tantalum or other dense materials–to protect onboard electronics and instrumentation.

As part of modifying the Cassini Prime Mission and designing the Cassini extended missions (referred to as the Equinox and Solstice Missions), a method for the placement of the groundtrack of a hyperbolic orbit over desired latitudes and longitudes was developed [1]. This method has been expanded and combined with prior design concepts [2,3] such that a number of flybys can be used to systematically cover a specific hemisphere of a moon.

2. Gravity Assist Trajectory Design

The enabling mechanism for complicated missions such as Galileo [4,5] and Cassini [6-8] is a concept understood for over a century and employed in a number of missions during the past forty years—the gravity assist. A gravity assist entails a spacecraft using a massive moving celestial body to significantly modify its trajectory. Depending on the flyby speed and distance, and how the spacecraft flies by the large gravitating body (above/below, behind/in-front), the spacecraft's orbit size (period, energy, and distance relative to the central body) and orientation (inclination and line of apsides relative to the central body to Sun line) can be altered in an incremental and predictable manner such that a wide range of geometries can be attained to meet myriad, often disparate, scientific goals.

2.1 Pump and Crank Angles

By the patched-conic assumption [2,9,10], the spacecraft's velocity relative the central body (v_{sc}) is given by the vector sum of the gravity assist body velocity (v_{ga}) and the spacecraft's v-infinity (v_∞) with respect to the gravity assist body. This sum is shown in Fig. 1.

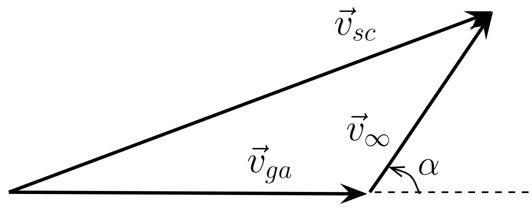

Figure 1: Pump angle.

The angle depicted in Fig. 1 is referred to as the *pump* angle (α). Applying the law of cosines, we may write the following equation for the pump angle:

$$v_{sc}^2 = v_\infty^2 + v_{ga}^2 + 2 v_\infty v_{ga} \cos(\alpha) \tag{1}$$

We may also use the *vis-viva* equation to transform Eq. 1 into a relation for the spacecraft's semi-major axis (a_{sc}) of its orbit relative to the central body. Here, r_{enc} is the *radius of encounter*, *i.e.*, the distance from the central body to the gravity assist body at the time of the gravity assist.

$$\frac{1}{a_{sc}} = \frac{2}{r_{enc}} - \frac{1}{\mu_{cb}} \left[v_\infty^2 + v_{ga}^2 + 2 v_\infty v_{ga} \cos(\alpha) \right] \tag{2}$$

This then also yields a relation for orbit period (T_{sc}) as a function of pump angle:

$$T_{sc} = 2\pi \sqrt{\frac{1}{\mu_{cb}} \left(\frac{2}{r_{enc}} - \frac{1}{\mu_{cb}} \left[v_\infty^2 + v_{ga}^2 + 2 v_\infty v_{ga} \cos(\alpha) \right] \right)^{-3}} \tag{3}$$

The velocity triangle in Fig. 1 can also be rotated out of the orbit plane of the gravity assist body when the spacecraft's orbit is inclined relative to the orbit of the gravity assist body. Figure 2 shows this, where the *crank angle* (κ) is used to describe the rotation of the velocity triangle out-of-plane. The basis in Figure 2 is defined by [11]:

$$\hat{q}_2 = \frac{\vec{v}_{ga}}{|v_{ga}|} \tag{4}$$

$$\hat{q}_3 = \frac{\vec{r}_{enc} \times \vec{v}_{ga}}{|\vec{r}_{enc}||\vec{v}_{ga}| \cos(\gamma_{ga})} \tag{5}$$

$$\hat{q}_1 = \hat{q}_2 \times \hat{q}_3 \tag{6}$$

where γ_{ga} is the flight path angle of the gravity assist body at the time of the encounter (this is zero for gravity assist bodies in circular orbits).

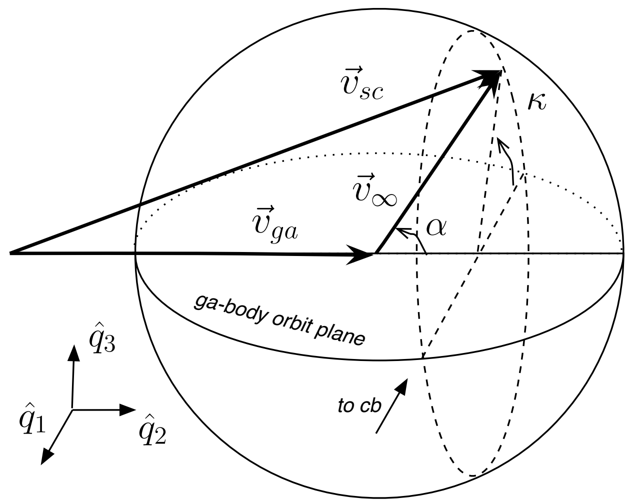

Figure 2: Crank angle.

The v-infinity vector in this reference frame is then given by:

$$\vec{v}_\infty = v_\infty \sin(\alpha)\cos(\kappa)\hat{q}_1 + v_\infty \cos(\alpha)\hat{q}_2 - v_\infty \sin(\alpha)\sin(\kappa)\hat{q}_3 \tag{7}$$

Let's introduce two more vector bases: a p-frame tied to the gravity assist body's orbit plane and an s-frame tied to the spacecraft's orbit plane:

$$\hat{p}_3 = \frac{\vec{r}_{enc} \times \vec{v}_{ga}}{|\vec{r}_{enc}||\vec{v}_{ga}|\cos(\gamma_{ga})} \tag{8}$$

$$\hat{p}_2 = \hat{p}_3 \times \hat{p}_1 \tag{9}$$

$$\hat{p}_1 = \frac{\vec{r}_{enc}}{|\vec{r}_{enc}|} \tag{10}$$

$$\hat{s}_1 = \frac{\vec{r}_{enc}}{|\vec{r}_{enc}|} \tag{11}$$

$$\hat{s}_3 = \frac{\vec{r}_{enc} \times \vec{v}_{sc}}{|\vec{r}_{enc}||\vec{v}_{sc}|\cos(\gamma_{sc})} \tag{12}$$

$$\hat{s}_2 = \hat{s}_3 \times \hat{s}_1 \tag{13}$$

The gravity assist body's velocity vector and the spacecraft's velocity vector are then given by:

$$\vec{v}_{ga} = v_{ga}\hat{q}_2 = v_{ga}\sin(\gamma_{ga})\hat{p}_1 + v_{ga}\cos(\gamma_{ga})\hat{p}_2 \tag{14}$$

$$\vec{v}_{sc} = v_{sc}\sin(\gamma_{sc})\hat{s}_1 + v_{sc}\cos(\gamma_{sc})\hat{s}_2 = v_{sc}\sin(\gamma_{sc})\hat{p}_1 + v_{sc}\cos(\gamma_{sc})\cos(i_{sc})\hat{p}_2 + v_{sc}\cos(\gamma_{sc})\sin(i_{sc})\hat{p}_3 \tag{15}$$

We may use these two equations to write the v-infinity in the p-frame:

$$\begin{aligned}\vec{v}_\infty &= \vec{v}_{sc} - \vec{v}_{ga} \\ &= [v_{sc}\sin(\gamma_{sc}) - v_{ga}\sin(\gamma_{ga})]\hat{p}_1 + [v_{sc}\cos(\gamma_{sc})\cos(i_{sc}) - v_{ga}\cos(\gamma_{ga})]\hat{p}_2 + v_{sc}\cos(\gamma_{sc})\sin(i_{sc})\hat{p}_3\end{aligned} \tag{16}$$

We can also transform Eq. 7 into the p-frame:

$$\begin{aligned}\vec{v}_\infty = {} & v_\infty[\sin(\alpha)\cos(\kappa)\cos(\gamma_{ga}) + \cos(\alpha)\sin(\gamma_{ga})]\hat{p}_1 + v_\infty[\cos(\alpha)\cos(\gamma_{ga}) - \sin(\alpha)\cos(\kappa)\sin(\gamma_{ga})]\hat{p}_2 \\ & - v_\infty\sin(\alpha)\sin(\kappa)\hat{p}_3\end{aligned} \tag{17}$$

Comparing Eqs. 16 and 17, the radial (p_1) components give a relation for the crank angle:

$$\cos(\kappa) = \frac{v_{sc}\sin(\gamma_{sc}) - v_{ga}\sin(\gamma_{ga}) - v_\infty\cos(\alpha)\sin(\gamma_{ga})}{v_\infty\sin(\alpha)\cos(\gamma_{ga})} \tag{18}$$

When the gravity assist body is in a circular orbit, this reduces to:

$$\cos(\kappa) = \frac{v_{sc}\sin(\gamma_{sc})}{v_\infty\sin(\alpha)} \tag{19}$$

Quadrant ambiguities in Eqs. 18 and 19 can be resolved by looking at the out-of-plane (p_3) components of Eqs. 16 and 17, which yields:

$$\mathrm{sign}(\kappa) = \mathrm{sign}(i_{sc}\cos(\gamma_{sc})) \tag{20}$$

2.2 Maximum Inclination

The p_3 component in Eqs. 18 and 19 yields a relation for the spacecraft's inclination with respect to the gravity assist body's orbit:

$$\sin(i_{sc}) = -\frac{v_\infty\sin(\alpha)\sin(\kappa)}{v_{sc}\cos(\gamma_{sc})} \tag{21}$$

Note that in the equation above, inclination can be negative. This corresponds to cases when the flyby is at the descending node of the spacecraft's orbit. Although, inclination is traditionally a strictly positive quantity, it is useful to allow it to go negative when talking about gravity assists, as otherwise separate relations for flybys at the ascending and descending nodes would need to be derived.

The p_2 component in Eqs. 18 and 19 yields a relation for the spacecraft flight path angle (γ_{sc}):

$$\cos(\gamma_{sc}) = \frac{1}{v_{sc}\cos(i_{sc})}[v_{ga}\cos(\gamma_{ga}) + v_\infty \cos(\alpha)\cos(\gamma_{ga}) - v_\infty \sin(\alpha)\cos(\kappa)\sin(\gamma_{ga})] \tag{22}$$

This can be combined with Eq. 21 to yield the following relation for spacecraft inclination:

$$\tan(i_{sc}) = v_\infty \sin(\alpha)\sin(\kappa)/\left[v_\infty \sin(\alpha)\cos(\kappa)\sin(\gamma_{ga}) - v_{ga}\cos(\gamma_{ga}) - v_\infty\cos(\alpha)\cos(\gamma_{ga})\right] \tag{23}$$

When $\gamma_{ga} = 0$, this reduces to:

$$\tan(i_{sc}) = -\frac{v_\infty \sin(\alpha)\sin(\kappa)}{v_{ga} + v_\infty \cos(\alpha)} \tag{24}$$

The maximum value of inclination happened when the crank is $\pm\pi/2$. Therefore the inclination is bounded by:

$$|\tan(i_{sc})| \leq \frac{v_\infty \sin(\alpha)}{v_{ga}\cos(\gamma_{ga}) + v_\infty\cos(\alpha)\cos(\gamma_{ga})} \tag{25}$$

The dependence on the pump angle in Eq. 25 means that each spacecraft orbit period will have an associated maximum inclination.

2.3. Flyby Groundtracks

If the gravity assist body is in a circular orbit, and tidally locked so the prime meridian always points towards the central body (true for almost all moons including Europa), the incoming or outgoing v-infinity can be written in terms of latitude (ϕ) and longitude (λ) in the p-frame:

$$\vec{v}_\infty = v_\infty[\cos(\phi)\cos(\lambda)\hat{p}_1 + \cos(\phi)\sin(\lambda)\hat{p}_2 + \sin(\phi)\hat{p}_3] \tag{26}$$

Equation 26 can be compared with Eq. 16 or Eq. 17 to give a latitude and longitude corresponding to a pump and crank angle or to a spacecraft inclination, semi-major axis, and flight-path angle. However, in doing so we must remember that the v-infinity vector on the inbound-asymptote is pointed towards the surface and we want to use the negative of the inbound v-infinity to find the point on the surface under the trajectory. If we do this we arrive at the following relations for the inbound latitude and longitude (ϕ_1,λ_1) and the outbound latitude and longitude (ϕ_2,λ_2) in terms of pump and crank before a flyby (α_1,κ_1) and after a flyby (α_2,κ_2).

$$\phi_1 = \operatorname{asin}(\sin(\alpha_1)\sin(\kappa_1)) \tag{27}$$

$$\lambda_1 = \operatorname{sign}(-\cos(\alpha_1))\operatorname{acos}(-\sin(\alpha_1)\cos(\kappa_1)/\cos(\phi_1)) \tag{28}$$

$$\phi_2 = \text{asin}(-\sin(\alpha_2)\sin(\kappa_2)) \tag{29}$$

$$\lambda_2 = \text{sign}(\cos(\alpha_2))\text{acos}(\sin(\alpha_2)\cos(\kappa_2)/\cos(\phi_2)) \tag{30}$$

The flyby's ground track is then a great circle connecting the inbound sub-point (ϕ_1,λ_1) to the outbound sub-point (ϕ_2,λ_2). The flyby periapsis occurs at the midpoint between these two (ϕ_p,λ_p), this is given by:

$$\phi_p = \phi_1 + \frac{1}{2}(\phi_2 - \phi_1) \tag{31}$$

$$\lambda_p = \lambda_1 + \frac{1}{2}(\lambda_2 - \lambda_1) \tag{32}$$

Note that in the above, (ϕ_p,λ_p) may need to be adjusted by $\pm 2\pi$ in order to get the regular quadrants for latitude and longitude.

2.4. Same-Body Transfers

Depending on the planetary system and a spacecraft's relative velocity with respect to the bodies in that system, one or more bodies exist that can be utilized for gravity assists. At Saturn and Uranus, Titan and Triton, respectively, are most easily utilized to design gravity assist tours. At Jupiter, the four Galilean moons, Io, Europa, Ganymede, and Callisto are all massive enough to be utilized. Apart from transfers between different moons, three basic* types of same-body transfers exist [2,11-13]: resonant, nonresonant, and pi-transfers.

A resonant transfer has a time-of-flight that is an integer multiple of the gravity assist body's period. Both flybys occur at the same point in the gravity assist body's orbit. Therefore, the spacecraft orbit plane is only constrained to contain the line connecting this point to the central body and the transfer may achieve a wide range of inclination. A resonant transfer is typically labeled as $m{:}n$, where m is the number of gravity assist body revolutions and n is the number of spacecraft revolutions during the transfer.

A nonresonant transfer's time-of-flight is not an integer multiple of the gravity assist body's orbit, and the flybys occur at different locations in the gravity assist body's orbit. In general, the two flybys and the central body do not fall on a line (except for pi-transfers) and the spacecraft inclination is constrained to be in the gravity assist body's orbit plane.

A pi-transfer is a special case of a nonresonant transfer where the time-of-flight of the transfer is m plus one-half times the gravity assist body's period. The flybys of a pi-transfer occur on a line passing through the central body, and hence these transfers can be inclined. In fact, they typically

* With large maneuvers or large third-body perturbations, leveraging transfers or other techniques are possible.

must be inclined with a specific inclination determined by the v-infinity magnitude [12]. A pi-transfer changes the location of the encounter by 180º.

2.5. Crank-over-the-top Sequence

Beginning from an equatorial orbit ($\kappa = 0$ or $\kappa = \pi$), a "crank-over-the-top" (COT) sequence [3] is defined as a set of resonant transfers (N) used to crank the spacecraft inclination up to a maximum inclination (i_{max}) for a given orbit period ($\kappa = \pi/2$), and continue cranking in the same direction—where the inclination will now decrease—until the spacecraft's orbit plane has returned to an equatorial orbit.

Figure 3 shows the geometry of one flyby of a COT sequence. Note that the incoming and outgoing v_∞ have the same pump angle, hence the flyby Δv is perpendicular to the moon velocity. Since the line of apsides of a flyby hyperbola is aligned with the flyby Δv, the flyby closest approach must lie in a plane perpendicular to the moon velocity and pass through the moon center of mass. Therefore, when a moon is tidally locked and in a circular orbit, the closest approach of a COT flyby occurs at 0^o or 180^o longitudes.

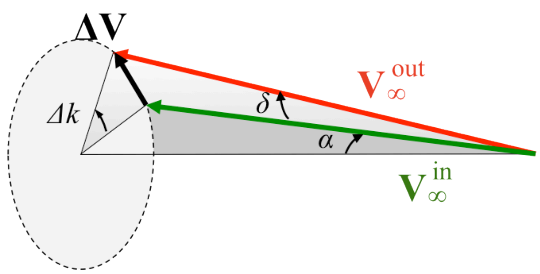

Figure 3: Geometry of one flyby in a COT sequence.

The flyby Δv can be written as,

$$\Delta v = 2v_\infty sin(\tfrac{\delta}{2}) \tag{33}$$

If the same period is maintained (i.e., no pumping), and the gravity assist is used to only crank, the flyby Δv can also be written as,

$$\Delta v = 2v_\infty sin(\alpha) sin(\tfrac{\Delta\kappa}{2}) \tag{34}$$

Using Eqs. 33 and 34, and by definition for a COT, $\Delta\kappa = \pi/N$, the flyby bending angle can be expressed as function of the pump angle and the number of COT flybys:

$$sin(\tfrac{\delta}{2}) = sin(\alpha) sin(\tfrac{\pi}{2N}) \tag{35}$$

Using the definition of the flyby bending angle:

$$sin(\tfrac{\delta}{2}) = \frac{\mu_{ga}}{\mu_{ga} + r_p v_\infty^2} \tag{36}$$

Equation 36 can be rearranged such that,

$$sin(\frac{\pi}{2N}) = (1 + \frac{r_p v_\infty^2}{\mu_{ga}})sin(\alpha) \tag{37}$$

where the pump angle is (re-arranging Eq. 3),

$$cos(\alpha) = \frac{\mu_{cb}(\frac{2}{r_{enc}} - \mu_{cb}(\frac{T_{sc}}{2\pi})^2)^{-1/3} - v_\infty^2 - v_{ga}^2}{2 v_{ga} v_{sc}} \tag{38}$$

Equations 37 and 38 can used to find the number of flybys of a COT given the flyby altitude, v-infinity and the resonance (*m:n*). Equations 37 and 38 can also be solved to find the required v-infinity for a given number of minimum-altitude flybys and a given resonance.

A COT sequence beginning with an inbound flyby will cover the sub-planet facing hemisphere of a tidally locked moon. At i_{max}, the flyby will occur at $\gamma_{sc} = 0°$ (periapsis when $T_{sc} < T_{ga}$, apoapsis when $T_{sc} > T_{ga}$, $e = 0$ when $T_{sc} = T_{ga}$) and all subsequent flybys will be outbound (referred to as an inbound-to-outbound COT, or I/O COT). Similarly, an O/I COT sequence beginning with outbound flybys will cover the anti-planet facing hemisphere of a tidally locked moon and will return to the equatorial plane with inbound flybys.

Figures 4 and 5 exhibit the characteristics of COT sequences at Europa, where the minimum altitude is 100 km. Specifically:

- For a given spacecraft orbit period (T_{sc}), the number of flybys (N) increases/decreases as the v-infinity increases/decreases (Fig. 4).
- For a given v-infinity, the number of flybys increases/decreases as the spacecraft orbit period decreases/increases (Fig. 5).

Figure 6 shows the parametric curves $P(v_\infty; N)$. For $N = 1$, a single gravity assist can flip the v-infinity from inbound to outbound (or vice versa), and is referred to as "v_∞-flipping." If the gravity assist body is in a circular orbit, a sequence of v_∞-flipping and non-resonant transfers can be used to change the location of the flyby on the moon's orbit. The resulting trajectory is periodic in the rotating frame defined by the moon and the planet. Figure 7 shows a 36 flyby v_∞-flipping sequence at Europa.

Lastly, as previously mentioned, when the same period resonant transfers are used throughout a COT sequence, all closest approaches will lie very near[†] the prime or 180º meridians (i.e., 90º away in longitude from gravity assist body's velocity vector). However, alternating the period of resonant transfers during a COT sequence (i.e., cranking *and* pumping), the closest approach can be placed away from the prime or 180º meridians (see Section 3.2).

[†] Libration and non-zero eccentricity will result in small closest approach deviations from 0º and 180º longitudes.

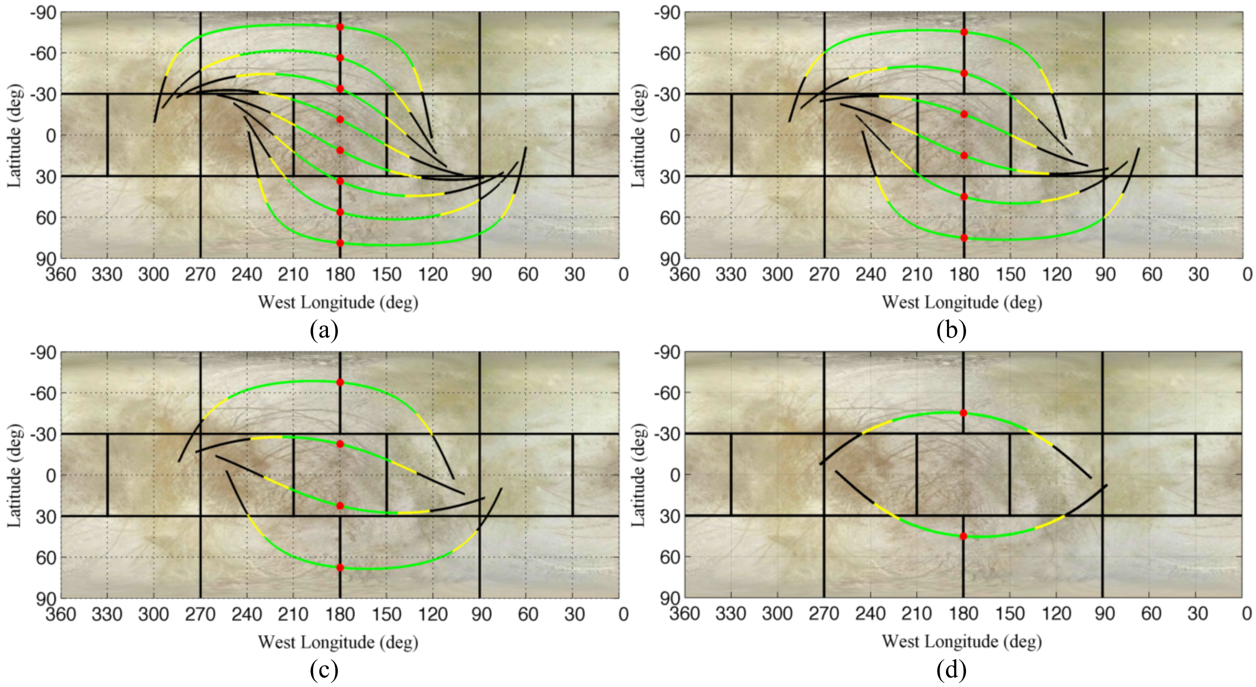

Figure 4: O/I COT sequences at Europa with constant period (14.2 days, 4:1 resonant transfer) and a v_∞ of: (a) 4.127 km/s, (b) 3.949 km/s, (c) 3.802 km/s, and (d) 3.702 km/s. Black: 1,000<alt<10,000 km; Yellow: 400<alt<1000 km; Green: alt≤400 km; Red: Closest approach.

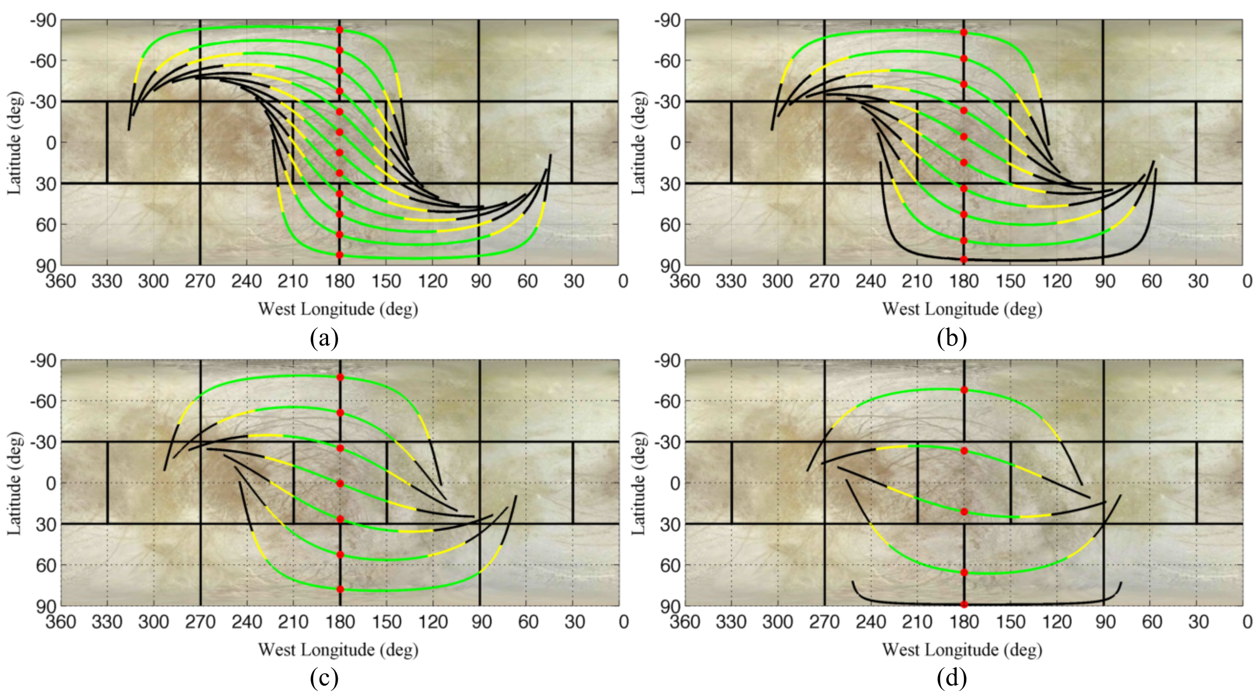

Figure 5: O/I COT sequences at Europa with constant v_∞ =4.266 km/s and varying period: (a) 10.65 days (3:1 resonance), (b) 14.2 days (4:1 resonance) (c) 17.75 days (5:1 resonance), and (d) 21.25 days (6:1 resonance). Black: 1,000<alt<10,000 km; Yellow: 400<alt<1000 km; Green: alt≤400 km; Red: Closest approach.

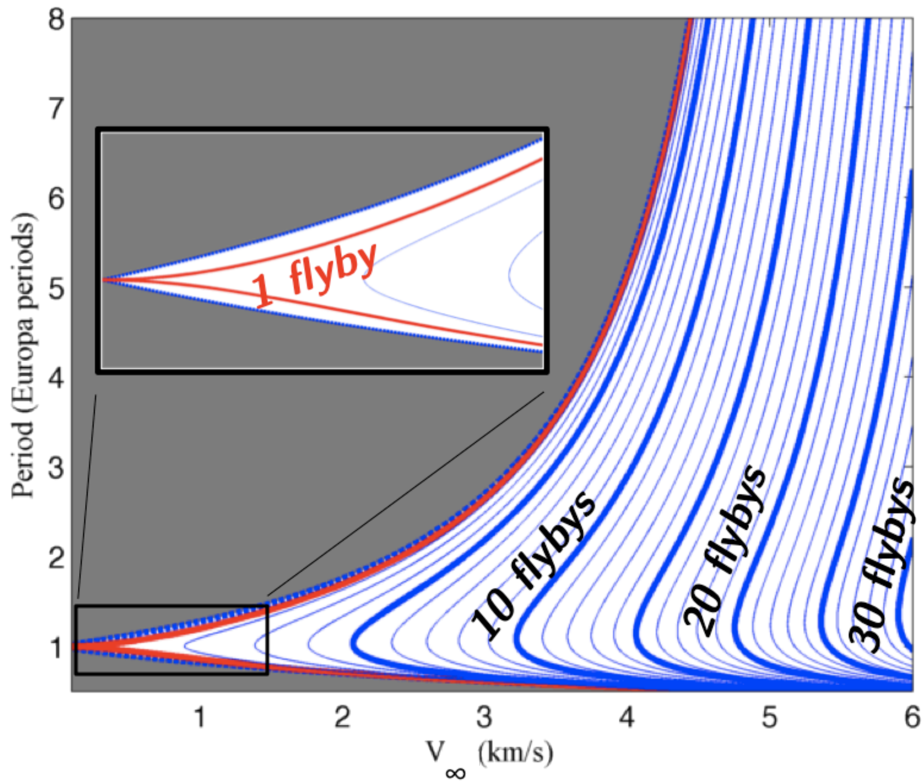

Figure 6: Number of flybys required by a COT sequence, as function of the period and of the v_∞. For $N = 1$, the graph shows the v_∞ flipping solutions.

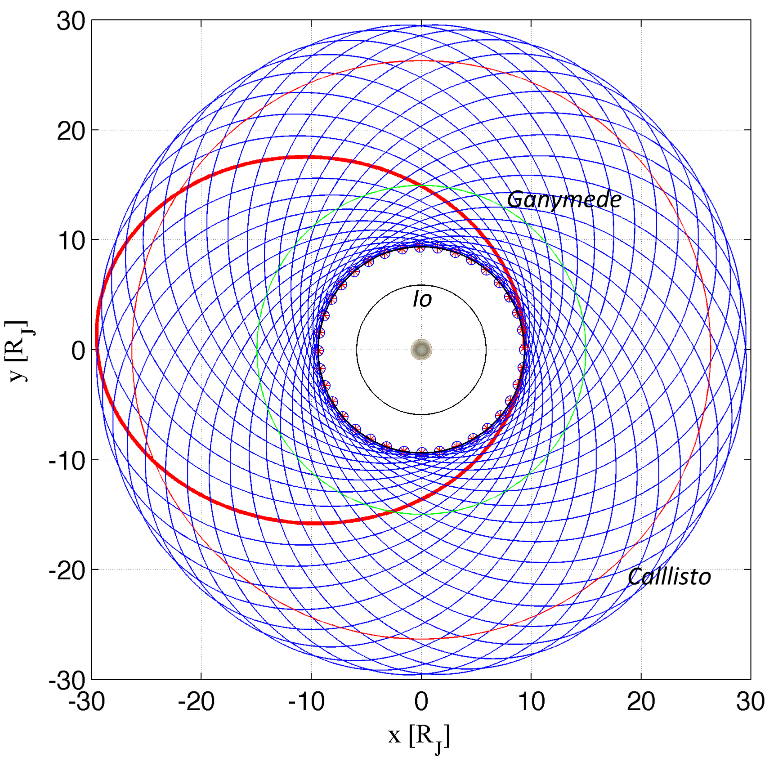

Figure 7: 3:1⁻ O/I non-resonant flyby v_∞-flipping example. v_∞ = 3.2 km/s, -10º regression in true anomaly per flyby. Rotates line of apsides ~360º using 36 flybys over 380 days.

3. Application

COT sequences can be used to obtain near global coverage for different moons in the solar system. The following two examples show the usefulness of these developed techniques, the latter showing that a multiple-flyby mission architecture can carry out a comprehensive investigation of Europa, exhibiting a number of potential advantages over an orbiter mission, and, is the preferred path by the scientific community to explore Europa under current fiscal constraints [14,15].

3.1 Titan Example

While Titan is one of the most fascinating moons in our solar system, it is also very useful in designing gravity assist trajectories at Saturn. For Cassini, given the high velocities the spacecraft encounters the various moons of Saturn, Titan is the only Saturnian satellite massive enough to significantly alter the spacecraft's trajectory. A single 1000 km altitude Titan flyby provides the spacecraft a gravity assist Δv in excess of 800 m/s. As a result, gravity assist tours are built as a sequence of Titan-to-Titan transfers, each flyby tuned to optimize not only Titan science, but also the science of the other four science discipline working groups on Cassini: Icy Satellites, Saturn, Rings, and Magnetosphere and Plasma.

During the development of the Cassini Solstice Mission, the following trajectory was built to exhibit to the Radar Team the amount of Titan coverage possible via two COT sequences (Fig. 8). Both COT sequences used 16 1:1 resonant transfers (T_{sc}=15.9 days); the first COT is an O/I COT sequence covering the anti-Saturnian hemisphere of Titan and occurs at Cassini's descending node. The second COT is an I/O COT sequence covering the sub-Saturnian hemisphere of Titan and occurs at Cassini's ascending node. Both COT sequences occur at the same Saturn local solar time (i.e., same location in Titan's orbit relative to the Saturn-Sun line), and since the Cassini radar uses microwaves to map Titan's surface, lighting conditions of the flybys were of no concern. Figure 9 shows the very three-dimensional nature and symmetric characteristics of COT sequences with relatively high v-infinities at a gravity assist body.

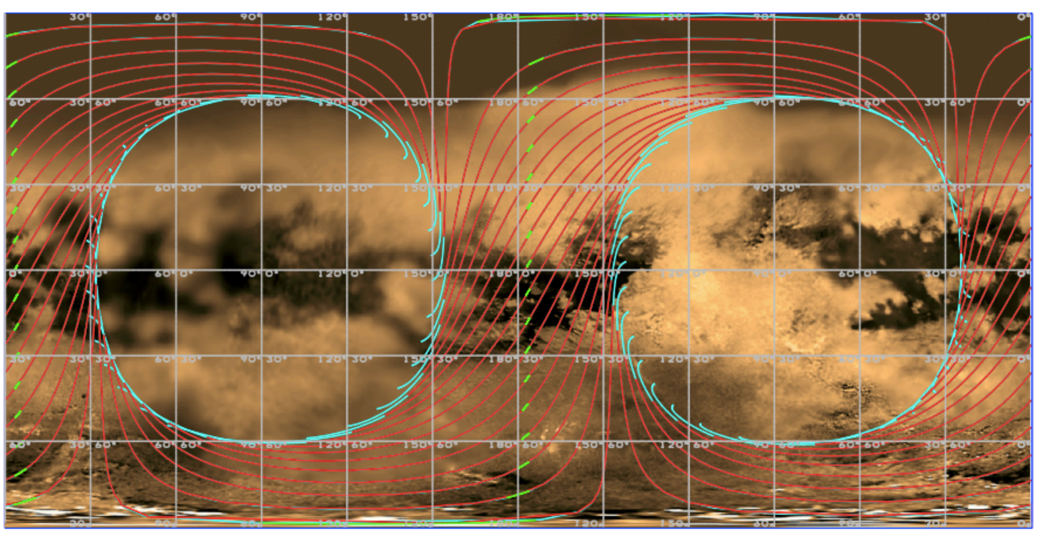

Figure 8: Nadir pointed groundtracks on Titan for two back-to-back COT sequences. Cyan: 10,000<alt<100,000 km; Red: 1000<alt<10,000 km; Green: Closest approach.

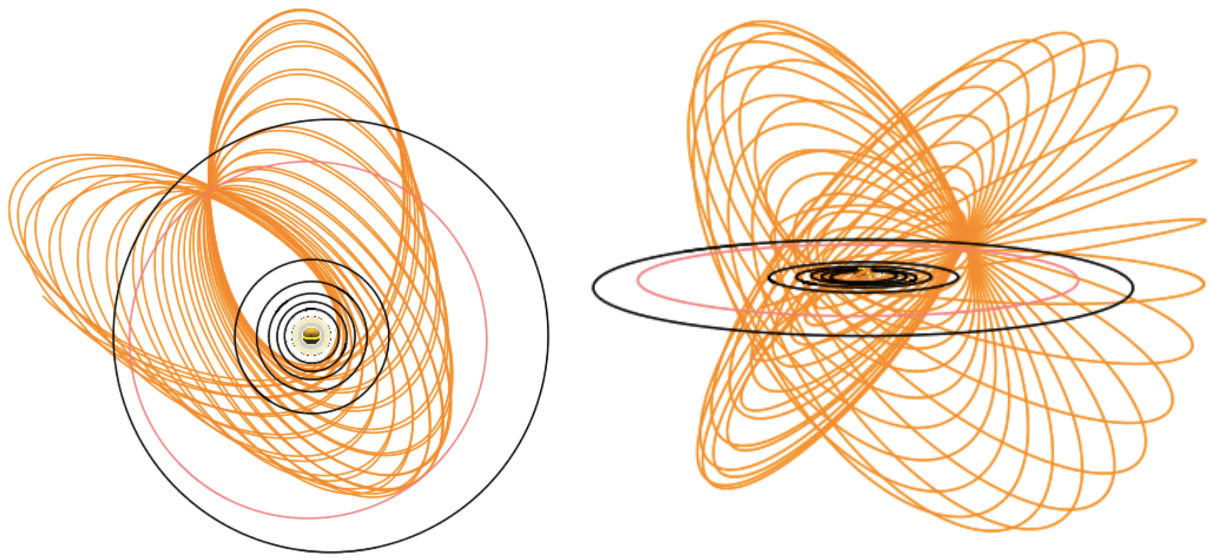

Figure 9: Two COT sequences using 1:1 resonant transfers with Titan (15.9 day period) with a v_∞ = 5.8 km/s. (a) View from Saturn N. pole (sun-fixed, towards top), (b) Oblique view (inertial). Orange: Spacecraft orbit; Red: Titan's orbit; Black: Orbit of six other inner icy satellites.

3.2 Europa Example

As reinforced by the 2011 NRC Decadal Survey [16], Europa remains one of the most scientifically intriguing targets in planetary science due to its potential suitability for life. However, based on JEO cost estimates and current budgetary constraints, the Decadal Survey recommended—and later directed by NASA Headquarters—a more affordable pathway to Europa exploration be derived. In response, a flyby-only proof-of-concept trajectory (referred to as 11-F5) has been developed to investigate Europa. See references 14 and 15 for a detailed description of the 11-F5 trajectory, and more generally, the proposed multiple-Europa flyby mission concept.

3.2.1 Science Objectives

The conceived model payload for a flyby-only Europa spacecraft contains an Ice-Penetrating Radar (IPR), Topographical Imager (TI), Shortwave Infrared Spectrometer (SWIRS), and an Ion and Neutral Mass Spectrometer (INMS). This notional payload is not meant to be exclusive of other measurements and instruments that might be able to meet the scientific objectives in other ways[‡]. Refer to the Europa 2012 Study Report [15] for the details mapping the specific instruments to their corresponding Europa investigations.

The following summarizes geometric constraints levied on the mission design in order to fulfill required scientific objectives for a compelling Europa multiple-flyby mission:

‡ NASA would ultimately select the payload through a formal Announcement of Opportunity (AO) process.

Ice Penetrating Radar (IPR)
- Closest approach (c/a) relative velocity: < 5 km/s
- c/a altitude: 100 km
- Coverage: Satisfy the following constraints in 11 of 14 panels (Fig. **10**)
  - Three 800 km groundtracks in anti-Jovian panels, and two 800 km groundtrack segments in each sub-Jovian panel (altitude ≤ 400 km)
  - Each groundtrack must intersect another groundtrack (intersection may be outside the panel of interest) below 1,000 km (when altimetry mode begins)
  - Cover anti-Jovian hemisphere first (preferred, not required)
- Requires *simultaneous* stereo imaging to provide topographic information necessary to process the IPR data

Topographic Imager (TI)
- c/a relative velocity: < 5 km/s
- c/a altitude: 100 km
- Solar phase: 50-70º (10-80º acceptable) when alt ≤ 400 km

Shortwave Infrared Spectrometer (SWIRS)
- c/a relative velocity: < 6 km/s
- c/a altitude: 100 km
- Local Solar Time: 9 am - 3 pm (the closer to noon the better)
- Solar phase angle: <45 degrees (preferred)
- Ability to target specific geologic features that are globally distributed (300 m/pixel, 11 of 14 panels)
- ≥ 70% coverage at ≤ 10 km per pixel

Ion and Neutral Mass Spectrometer (INMS)
- c/a relative velocity: < 7 km/s
- c/a altitude: 25 km (or more generally, as close as navigationally possible)

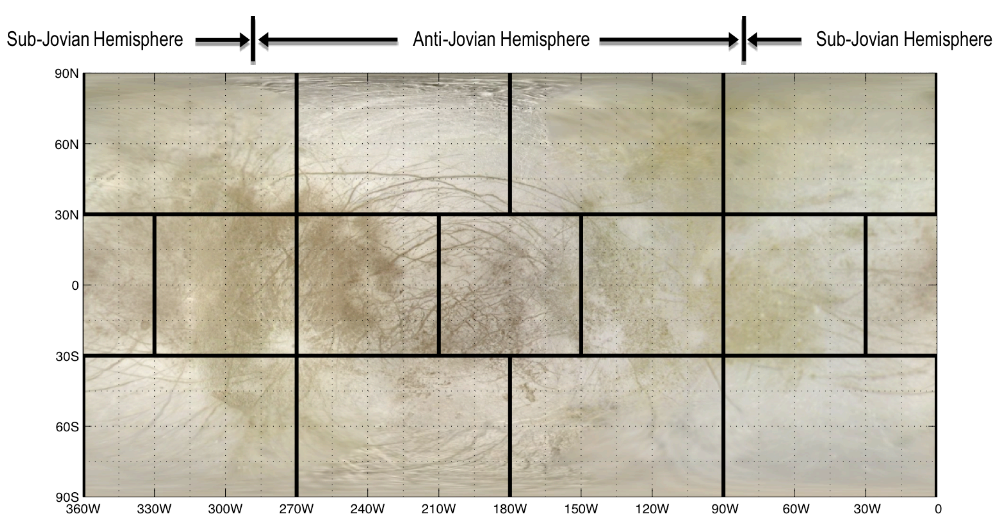

Figure 10. 14 panels defined by the Science Definition Team (SDT) used to assess global-regional coverage. Since Europa is tidally locked, the same hemispheres always face towards (sub-Jovian) or away from (anti-Jovian) Jupiter.

3.2.2 Multiple-Flyby Trajectory (11-F5)

The 11-F5 trajectory is a fully integrated trajectory from Earth launch (2021) through a notional end-of-mission (Ganymede impact). The Jovian tour consists of 34 Europa and 8 Ganymede flybys over the course of 2.4 years, reaches a maximum Jovicentric inclination of 14.9º, has a deterministic ΔV of 157 m/s (post–PJR), and has a TID[§] of 2.0 Mrad. The trajectory design goal was to maximize IPR, TI, SWIRS and INMS coverage while minimizing TID, mission duration (and hence operations costs), and ΔV.

After a 6.37-year Venus-Earth-Earth gravity assist (VEEGA) interplanetary trajectory, five Ganymede flybys (including Ganymede-0 prior to JOI) would be used to lower the spacecraft's orbital energy with respect to Jupiter and set up the correct flyby conditions (lighting and relative velocity) at Europa. First, since Europa is tidally locked, the terrain illuminated by the Sun is simply a function of where Europa is in its orbit. By implementing a nonresonant G0–G1 transfer followed by three outbound resonant transfers, the spacecraft's line of nodes can be rotated clockwise such that the first set of Europa flybys would occur very near the Sun–Jupiter line, and hence, Europa's anti-Jovian hemisphere would be sunlit. This is necessary since visible wavelength stereo imaging must be done in unison with IPR measurements as outlined in Section 3.2.1. Second, to meet the science coverage requirements, but also minimize the number of Europa flybys (and hence minimize TID), an O/I COT sequence (COT-1) would use a combination of 4:1 (T_{sc}=14.3 days) and 7:2 (T_{sc}=12.4 days) resonant transfers with a v_∞ of approximately[**] 3.9 km/s. While alternating between the two resonances takes more time and leads to a higher TID (7:2 resonance has two perijove passages between Europa flybys) as opposed to using only 4:1 resonant transfers, it would result in the closest approaches being pulled away from the 180º meridian far enough to place a large portion of the groundtrack in the equatorial leading and trailing sectors of the anti-Jovian hemisphere (Fig. 11).

Once COT-1 is complete, a nonresonant Europa transfer would be used to get back to an outbound flyby such that another O/I COT sequence could be implemented to cover the anti-Jovian hemisphere of Europa again. This nonresonant transfer would also change the local solar time (LST) of the Europa flybys.

All flybys in COT-1 occur at the ascending node. COT-2 (using strictly 4:1 resonant transfers) instead cranks in the opposite direction, placing the flybys at the descending node. This results in the COT-2 groundtracks intersecting the COT-1 sequence groundtracks (instead of running nearly parallel), hence fulfilling the IPR requirements in all seven anti-Jovian hemisphere sectors to have groundtracks with intersections (Fig. 12).

Before IPR, TI and SWIRS data could be collected on Europa's sub-Jovian hemisphere, the observational lighting conditions need to be changed by 180º. That is, the location of the Europa flybys needs to be moved to the opposite side of Jupiter so that Europa's sub-Jovian hemisphere would be sunlit. To do this, a "switch-flip" was implemented [14]. A switch-flip involves first cranking up the inclination and pumping down the orbit period with Europa flybys to set up the correct geometry for a Europa-to-Ganymede pi-transfer. Next, a Ganymede pi-transfer is

[§] Total ionizing dose Si behind a100-mil Al, spherical shell.
[**] Variations in v_∞ occur due to Europa's eccentricity and apsidal precession.

executed (3.5-day time-of-flight), followed by a 1:1 resonant Ganymede transfer that would crank down the inclination to set up the final transfer, a Ganymede-to-Europa pi-transfer. The result: All subsequent Europa flybys are located ~180º away from the last Europa flyby in COT-2 and the sub-Jovian hemisphere of Europa is sunlit.

Immediately following the Ganymede-to-Europa transfer, Europa flybys would be used to pump-up the orbit and crank-over-the-top. Like COT-1, the goal of COT-3 (I/O) is to minimize the number of flybys while still providing adequate coverage for science. However, since the v_∞ is ~3.5 km/s (instead of 3.9 km/s in COT-1), the COT-3 sequence would need to instead alternate between 3:1 (T_{sc}=10.7 days) and 5:2 (T_{sc}=8.8 days) resonant transfers to accomplish this. Lastly the first four Europa flybys in COT-3 (Europa27–Europa30) would be in Jupiter's shadow; hence no stereo imaging can be performed in unison with IPR measurement (Fig. 13). This is something that wasn't noticed during the design of the 11-F5 trajectory, but will be corrected in next iteration of tour design.

Once COT-3 is complete, a nonresonant Europa transfer would be used to get back to an inbound flyby such that another I/O COT sequence can be implemented to cover Europa's sub-Jovian hemisphere.

Finally, COT-4 (I/O) cranks in the opposite direction from COT-3 (i.e., switches the node at the Europa flybys from descending to ascending) with 3:1 resonant transfers to intersect the COT-3 sequence groundtracks, fulfilling the IPR requirements in six of the seven sub-Jovian hemisphere sectors (Fig. 13).

At the conclusion of COT-4, 13 of the 14 sectors have been covered sufficiently to meet the observational and measurement requirements of all four instruments on board as defined by the SDT. Figures 14-16 show the cumulative topographic imaging coverage, petal plot, and the network of flyby around Europa.

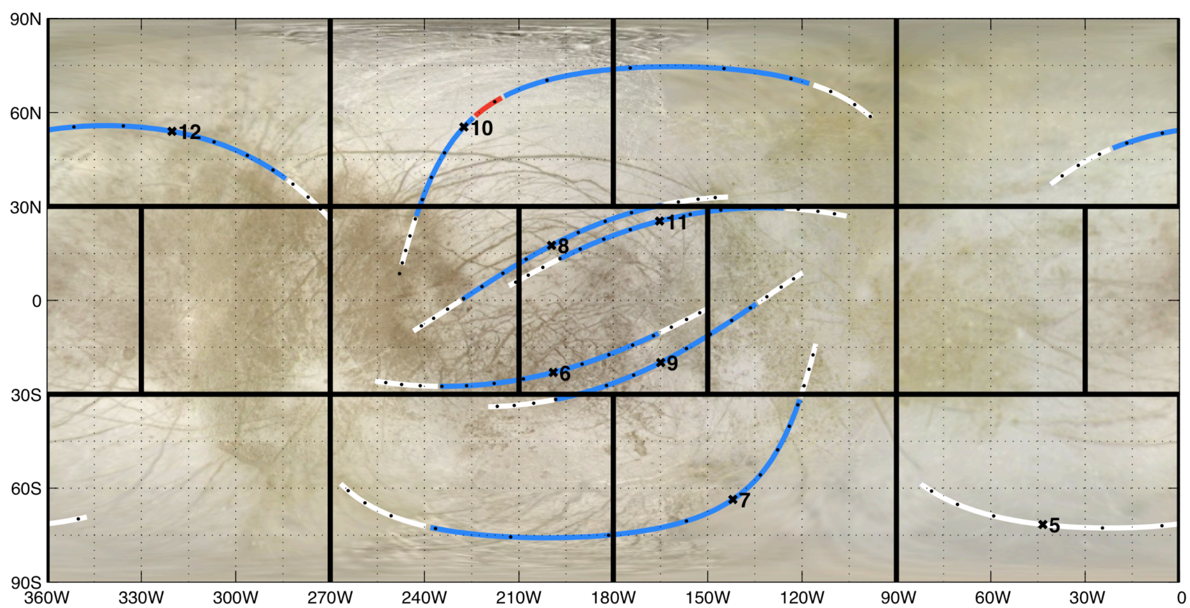

Figure 11. Europa COT-1 (O/I) nadir groundtracks. Closest approach is marked with an "x"; Red: 0<alt≤25 km; blue: 25<alt<400 km; white: 400<alt<1,000 km.

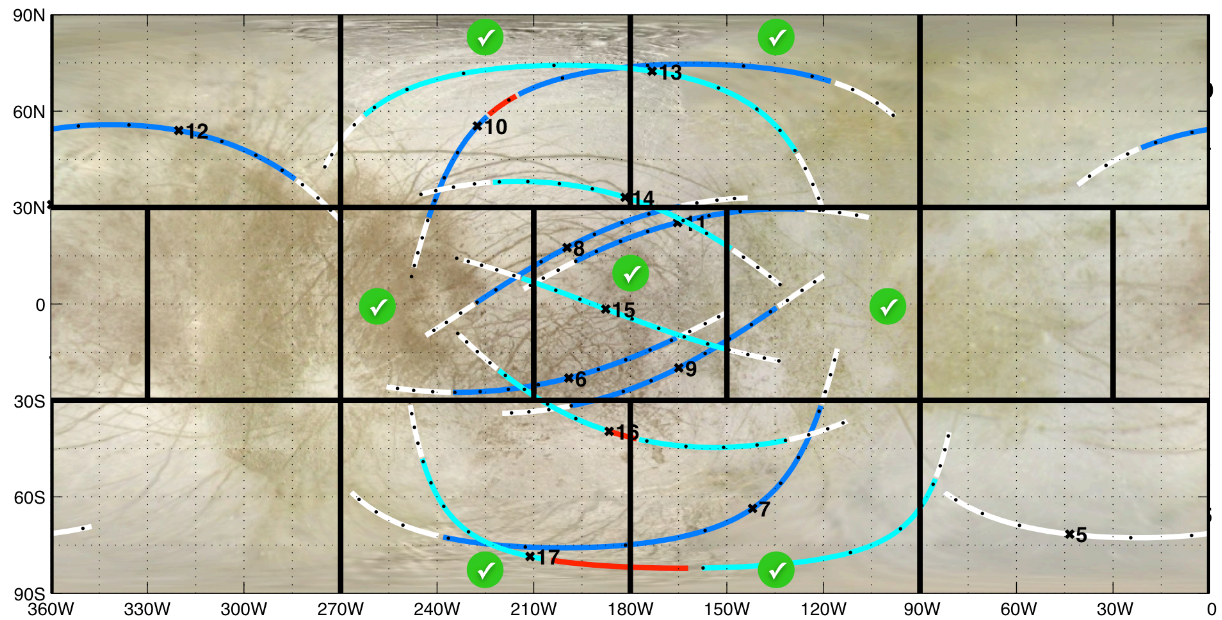

Figure 12. Europa COT-1 (O/I) and COT-2 (O/I) nadir groundtracks. Green check marks: IPR requirements are met; Closest approach: Marked with an "x"; Red: 0<alt≤25 km; blue (COT-1) and cyan (COT-2): 25<alt<400 km; white: 400<alt<1000 km.

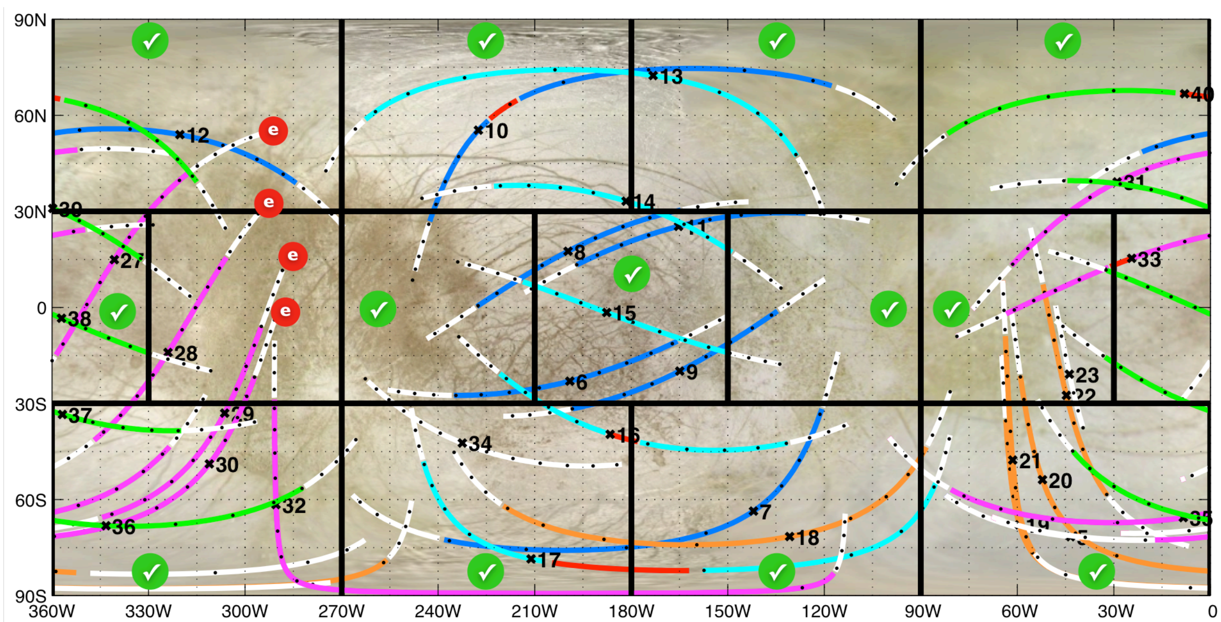

Figure 13. Europa nadir groundtrack plot for entire 11-F5 trajectory. Green check marks: IPR requirements are met; Red circles with "e": flybys in eclipse; Closest approach: Marked with an "x"; Red: 0<alt≤25 km; blue (COT-1), cyan (COT-2), orange (switch-flip), magenta (COT-3), and green (COT-4): 25<alt<400 km; white: 400<alt<1000 km.

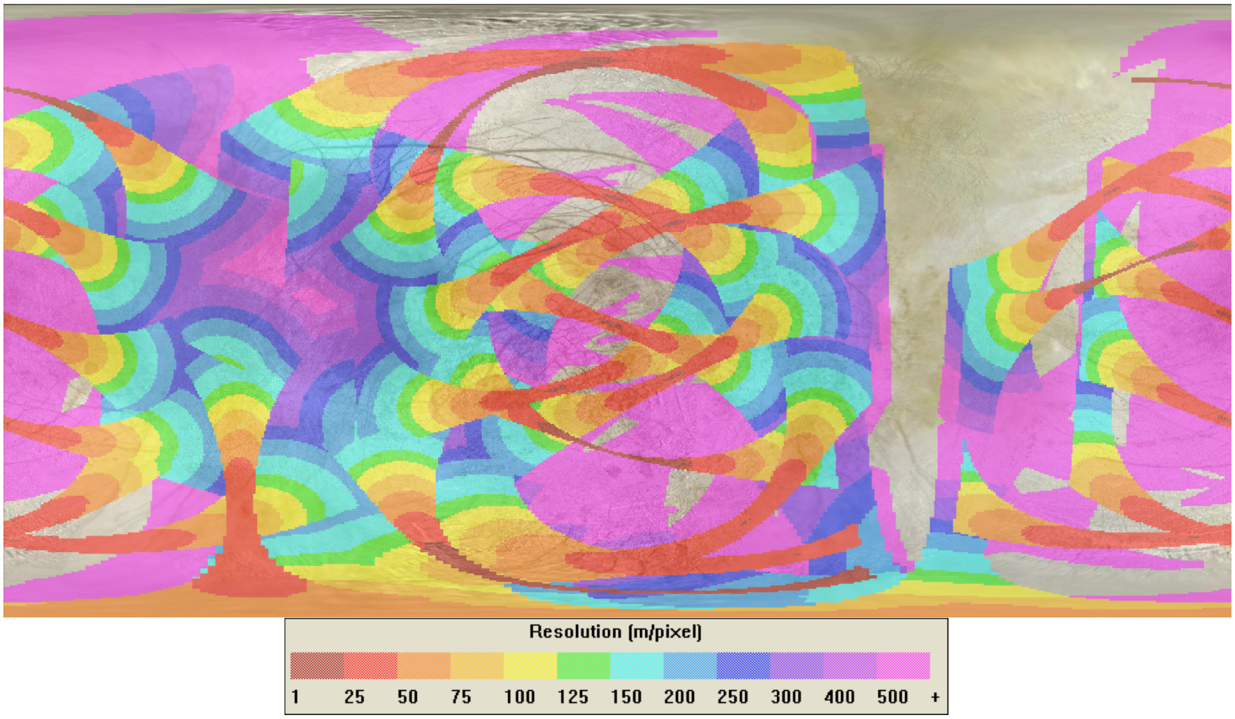

Figure 14. Nadir pointed cumulative topographic stereo imaging map for altitudes ≤ 4,000 km and solar incidence angles between 0-90º. Figure provided by Erick Sturm.

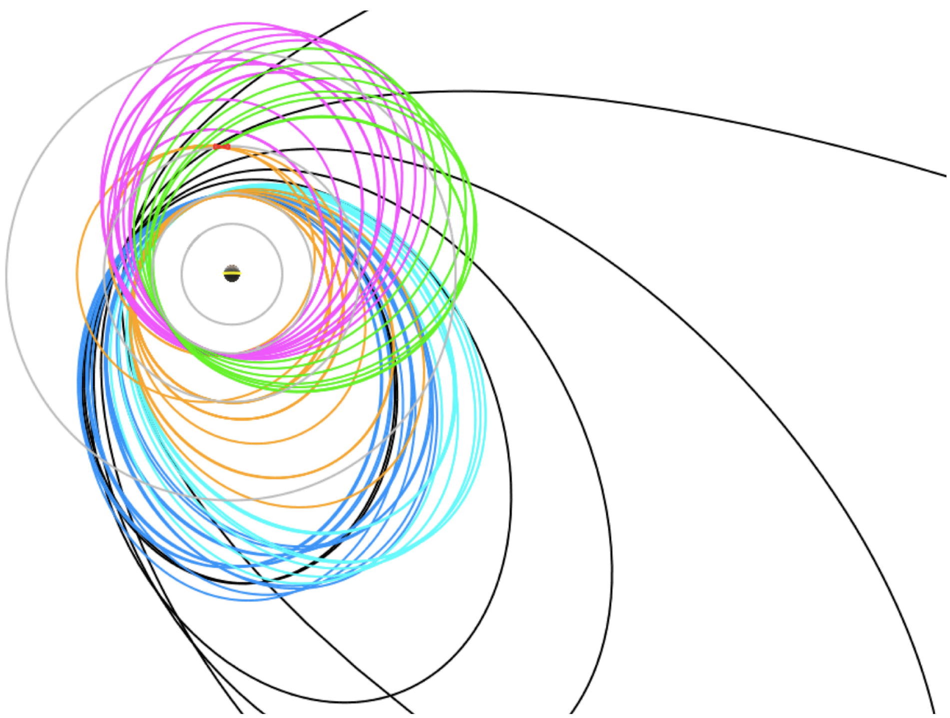

Figure 15. 11-F5 Petal Plot. View from Jupiter's north pole (Sun-fixed, towards top). Black: pump-down; blue: COT-1; cyan: COT-2; orange: switch-flip; magenta: COT-3; green COT-4; gray: orbits of the four Galilean satellites.

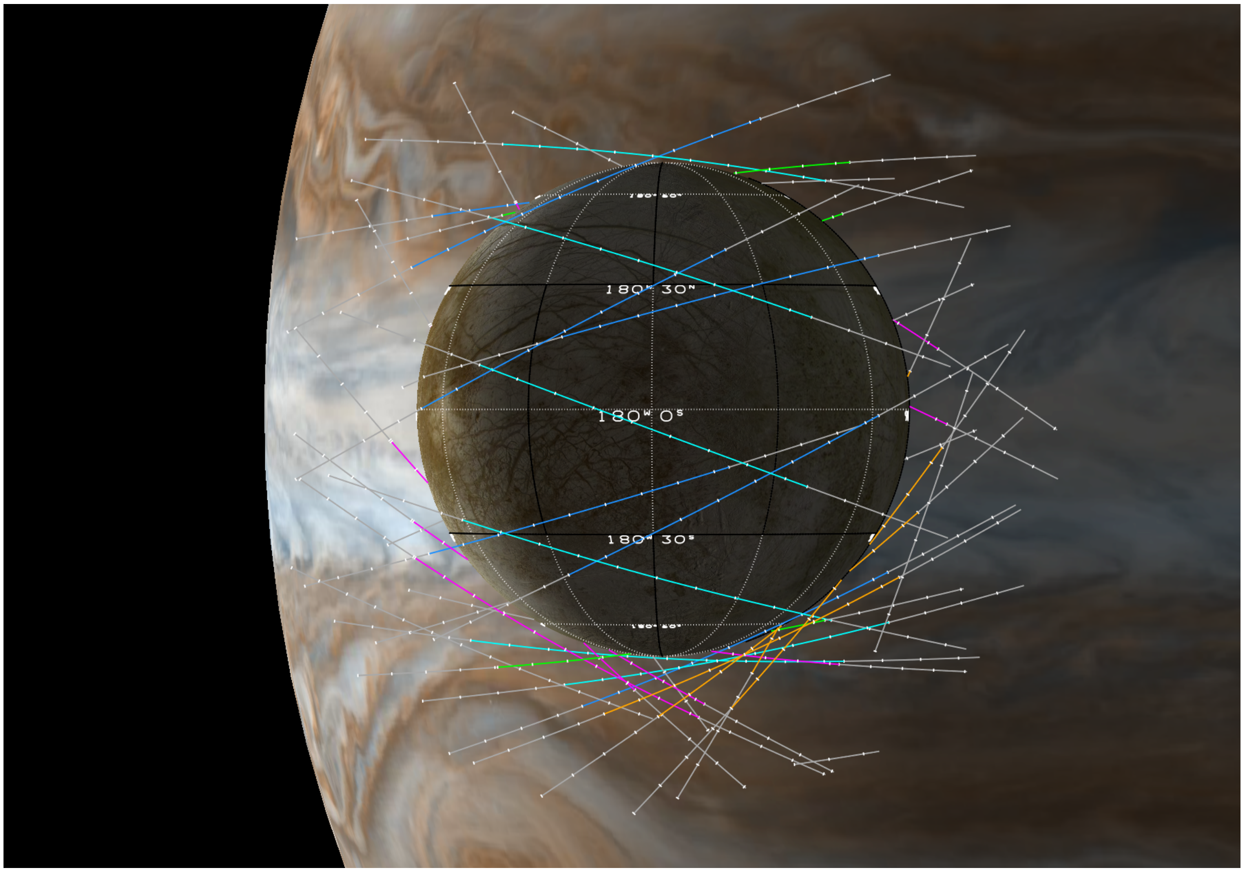

Figure 16. Global-regional coverage via multiple Europa flybys.

3.2.3 Multiple-Flyby Advantages

A variety of scientific investigations are required to address and answer key questions about Europa's habitability. For a given launch vehicle such as the Atlas V 551 (or smaller), a multiple-flyby mission can exhibit many potential advantages over an orbiting spacecraft including:

- Given the finite capability of a chosen launch vehicle, more mass is available for scientific instrumentation and electronic component shielding (effectively increasing the lifetime of the mission) by forgoing EOI (i.e., the large amount of propellant needed to dissipate the spacecraft's energy such that Europa orbit is reached)

- The ability to utilize a "store and forward" approach (i.e., collect, store, and eventually downlink data) enabling the use of higher power instruments in the vicinity of Europa since the spacecraft would never have to simultaneously operate the instruments and a high power telecom system

- The large amount of time the spacecraft would spend away from Europa (in Jupiter orbit) would allow ample time to downlink the large amounts of data collected during each flyby without accumulating radiation dosage

- Data return is less susceptible to spacecraft or DSN anomalies due to much less compressed/stressed operations at Europa

- Since the spacecraft is not constrained to permanently residing in Europa's gravity well, new Jupiter system campaigns could be executed once the spacecraft expected TID limits are reached (i.e., similar global-regional coverage campaigns at Ganymede and/or Callisto)

- The mission has many spacecraft disposal options [14], none of which include Europa impact

4. Conclusions

A trajectory design strategy to obtain near global coverage of one or more moons in a system via multiple flybys has been developed. This strategy was used to design a complex network of 34 Europa flybys to efficiently investigate the habitability of Europa—previously thought infeasible—and has uncovered that a multiple-flyby mission architecture exhibits a number of potential advantages over an orbiter mission. This developed multiple-flyby Europa mission is now the preferred path by the scientific community to explore Europa in the near future given current fiscal constraints, and, the quality and the quantity of science return that is desired.

Acknowledgments

This research was carried out at the Jet Propulsion Laboratory, California Institute of Technology, under a contract with the National Aeronautics and Space Administration (NASA). Reference to any specific commercial product, process, or service by trade name, trademark, manufacturer or otherwise, does not constitute or imply its endorsement by the United States Government or the Jet Propulsion Laboratory, California Institute of Technology.

References

[1] Buffington, B., and Strange, N., "Science Driven Design of Enceladus Flyby Geometry", 57th International Astronautical Congress 2006, Paper IAC-06-C1.6.05, Valencia, Spain, October 2-6, 2006.

[2] Uphoff, C., Roberts, P. H. and Friedman, L. D., "Orbit Design Concepts for Jupiter Orbiter Missions", AIAA Mechanics and Control Conference, AIAA Paper 74-781, Anaheim, California, Aug. 1974.

[3] Wolf, A.A., "High-Inclination Orbit Sequences for Cassini Tours", Internal JPL Presentation, Feb. 2, 1996.

[4] Diehl, R. E., Kaplan, D. I., and Penzo, P. A., "Satellite Tour Design for the Galileo Mission," AIAA Aerospace Sciences Meeting, AIAA Paper 83-0101, Reno, Nevada, Jan. 1983.

[5] Wolf, A.A., "Touring the Saturnian System," Space Science Reviews, Vol. 104, 2002, pp. 101-128.

[6] Strange, N., Buffington, B., and Jones, J.B., "In-Flight Trajectory Changes to the Cassini-Huygens Prime Mission," AIAA/AAS Astrodynamics Specialist Conference, Honolulu, HI, AIAA Paper 2008-6750, August 19-23 2007.

[7] Buffington, B., Strange, N., and Smith, J., "Overview of the Cassini Extended Mission Trajectory," AIAA/AAS Astrodynamics Specialist Conference, Honolulu, HI, AIAA Paper 2008-6752, August 18-21 2008

[8] Smith, J., and Buffington, B., "Overview of the Cassini Solstice Mission Trajectory," AAS/AIAA Astrodynamics Conference, AAS Paper 09-351, Pittsburg, PA, Aug. 2009.

[9] Broucke, R.A., "The Celestial Mechanics of Gravity Assist," AIAA/AAS Astrodynamics Conference, AIAA Paper 88-4220, Minneapolis, Minnesota, Aug. 1988.

[10] Cesarone, R.J., "A Gravity Assist Primer," AIAA Student Journal, Vol. 16, Spring 1989, pp. 16-22.

[11] Strange, N., Russell, R., and Buffington, B., "Mapping the V-infinity Globe," AAS/AIAA Astrodynamics Specialists Conference, AAS Paper 07-277, Mackinac Island, MI, August 19-23, 2007.

[12] Strange, N., and Sims, J., "Methods for the Design of V-Infinity Leveraging Maneuvers", AAS/AIAA Astrodynamics Specialist Conference, AAS Paper 01-437, Quebec, Quebec, August 2001.

[13] Buffington, B., and Strange, N., "Patched-Integrated Gravity Assist Trajectory Design," AAS /AIAA Astrodynamics Specialist Conference, Mackinac Island, MI, AAS Paper 07-276, August 19-23 2007.

[14] B. Buffington, S. Campagnola, and A. E. Petropoulos, "Europa Multiple-Flyby Trajectory Design," AIAA/AAS Astrodynamics Specialist Conference 13 - 16 August 2012, Minneapolis, Minnesota, No. AIAA 2012-5069, August 2012.

[15] Europa Study Team, Europa Study 2012 Report, JPL D-71990, May 01, 2012, http://solarsystem.nasa.gov/europa/-2012study.cfm.

[16] Space Studies Board, "Visions and Voyages for Planetary Science in the Decade 2013–2022", The National Academies Press, Washington, DC (2011).